Medium Effect on the Rotational Isomerism in 1,3,5-Triacetylbenzene

Aleksandra Konopacka[1], **Joanna Pająk**[2], **Guido Maes**[2], and **Zbigniew Pawełka**[1,*]

[1] Faculty of Chemistry, University of Wrocław, Wrocław, Poland

[2] Department of Chemistry, University of Leuven, Heverlee, Belgium

Summary. The optimal geometries, energies, polarities, infrared frequencies, and intensities of the non-polar and polar conformers of 1,3,5-triacetylbenzene were calculated using DFT/*B3LYP*/6-311G** and semi-empirical (AM1 and PM3) methods. All the methods revealed that the non-polar conformer prevails in vacuum. The infrared spectra in the solid state, in Ar matrix, and in liquid solutions as well as the dipole moments of 1,3,5-triacetylbenzene in many solvents show the distinct influence of the environment on the non-polar conformer ⇌ polar conformer equilibrium. The effect of solvent polarity on the standard *Gibbs* energy of this conformational equilibrium is quantitatively discussed in terms of the continuum-homogenous dielectric model.

Keywords. 1,3,5-Triacetylbenzene; Conformational equilibrium; DFT calculations; Dipole moments; Infrared spectra; Solvent effect.

Introduction

1,3,5-Triacetylbenzene (**1**) exists in different rotational states, of which two conformers, denoted further as **1a** (non-polar form, point group C_{3h}) and **1b** (polar form, point group C_s), are stable. These point groups correspond to configurations in which one hydrogen atom of the methyl group lies in the plane of the molecule and the remainder are arranged symmetrically. In the isolated state (in vacuum) the non-polar **1a** conformer should prevail over **1b**. On the other hand, due to the high polarity of the **1b** form, its stabilization in a polar environment maybe

expected [1]. The experimental data referring to the conformational behavior of **1** in condensed phases are, however, scattered. A detectable increase in the dipole moment of **1** in benzene solution with increasing temperature (2.31 D at 14.2°C and 2.79 D at 57.9°C) has been observed [2]. This tendency indicates that with increasing temperature, the **1a** ⇌ **1b** equilibrium is shifted to the right and $\Delta H°$ of this process is positive. A neutron diffraction investigation [3] of the crystal structure of **1** has been performed together with X-ray diffraction analysis [4]. For our interests, the extent of the molecular symmetry of **1** is important. The molecule, being a polar form, belongs to the C_1 point group. Its interesting molecular feature is the deviation of the oxygen and methyl carbon atoms from the central plane. The non-hydrogen atoms of the acetyl group and the ring carbon to which the $COCH_3$ group is bonded form a planar array inclined with respect to the central plane. The average torsion angle is 8.8°. Thus, the molecule possesses a slightly propeller-like form. On the other hand, the infrared spectra of **1** in solid samples and in solution have been interpreted as arising from the non-polar **1a** conformer of C_3 symmetry [5]. The above scanty data and our persistent interest in various manifestations of the internal rotation of the acetyl and formyl groups [6–9] encouraged us to perform the conformational analysis of **1** in vacuum, in Ar matrix, and in liquid solutions of different polarity. First, the optimized geometries, energies, and polar and infrared properties of the **1a**

* Corresponding author. E-mail: zp@wchuwr.chem.uni.wroc.pl

and **1b** conformers were calculated using the density functional theory (*B3LYP*) combined with the 6-311G(d,p) basis set. The DFT results, in particular the dipolar ones, were compared with those yielded by the semi-empirical (AM1 and PM3) methods. To establish the solvent influence on the rotational conformerism, the dipole moments of **1** in solvents with dielectric permittivities varying from $\varepsilon = 2.228$ to 10.36 were determined. The dipolar data were supported by infrared spectra of **1** in the solid state, in Ar matrix, and in various solvents with hope to distinguish directly both conformers. Both the dipolar and infrared methods allowed us to estimate the standard *Gibbs* energy, ΔG°, of the conformational equilibrium (see Scheme 1). In our foregoing papers, theoretical studies of benzaldehydes and acetophenones conducted towards their conformational behavior have shown a good concordance with the experimental data in solutions after assumption of appropriate solvation models [6–9]. In this paper, the effect of dipole solvation on the $\mathbf{1a} \rightleftharpoons \mathbf{1b}$ equilibrium is quantitatively discussed in terms of the continuum – homogeneous dielectric model.

1a   **1b**
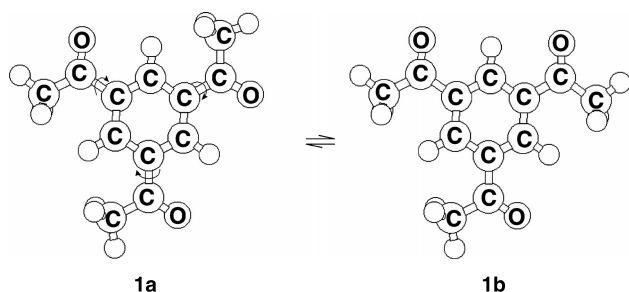
Scheme 1

Results and Discussion

Conformation of 1,3,5-Triacetylbenzene in Vacuum

The theoretical results pertinent to the rotational isomerism in **1** are given in Table 1. The interesting spectroscopic features of this isomerism will be presented further in Table 3. All the methods reveal both stable conformers of **1** to be planar. Thus, the polar conformer's observed deviation from planarity in the crystalline state [3] is due to lattice effects. The differences in conformational energies estimated by the DFT and semi-empirical methods are in the range between 4.90 and 7.61 kJ/mol. The molar ratio, $x_{\mathbf{1b}}$, calculated from the *Boltzmann* distribution function, are of the order of 0.1. This leads, in spite of the high polarity of the **1b** form, to the low dipole moment values of **1** in vacuum (see Table 2). On the other hand, such a large difference in the polarities of the two conformers suggests that the energetic gap between them can be overcome by the electrostatic interaction of the **1b** form with the environment. Thus, one could expect that in more

Table 1. Conformational energies, dipole moments, and populations of the **1b** conformer of 1,3,5-triacetylbenzene in vacuum

Method	$\Delta E^{*}/\mathrm{kJ\,mol^{-1}}$	$\mu_{\mathbf{1b}}/\mathrm{D}$	$x_{\mathbf{1b}}$
PM3	4.90	4.21	0.122
AM1	5.69	4.43	0.092
DFT/*B3LYP*/6-311G**	7.61	4.43	0.044

* $\Delta E = E_{\mathbf{1b}} - E_{\mathbf{1a}}$; $\quad E_{\mathbf{1b}}(\mathrm{DFT}) = -1812020.67\,\mathrm{kJ/mol}$; $E_{\mathbf{1b}}(\mathrm{PM3}) = -240034.82\,\mathrm{kJ/mol}$; $E_{\mathbf{1b}}(\mathrm{AM1}) = -256891.41\,\mathrm{kJ/mol}$

Table 2. Calculated and experimental dipole moments of 1,3,5-triacetylbenzene (**1**) in vacuum and various solvents

Medium	$\alpha\varepsilon_1$	β	γn_1^2	μ/D	μ/D acetophenone [7]
Vacuum					
PM3				1.47	2.79
AM1				1.34	2.97
DFT				0.93	3.02
CCl$_4$	6.576	−0.4909	0.4848	2.24	3.01
C$_2$Cl$_4$	6.821	−0.5081	0.2534	2.32	–
1,4-Dioxane	12.059	0.3908	1.0044	2.87	2.92
Benzene	9.585	0.7111	0.4560	2.56	2.92
Mesitylene	5.254	0.4026	0.1334	2.40	–
Trichloroethylene	9.633	−0.3907	0.4561	2.63	–
1,2-Dibromoethane	10.897	−0.9285	0.1796	2.81	–
1-Chlorobutane	9.139	0.5603	0.7441	3.25	2.95
1,2-Dichloroethane	10.592	−0.1691	0.6876	3.56	–

polar solvents, conformer **1b** will become predominant. Therefore our aim was to use further experimental dipole moments and infrared spectra to investigate the solvent (phase)-induced shifts in the **1a** ⇌ **1b** conformational equilibrium.

Dipole Moments of 1,3,5-Triacetylbenzene

The dipole moments of **1** in different environments are collected in Table 2. Knowing the population and calculated dipole moment of the **1b** form (see Table 1), the average dipole moments of **1** in vacuum were estimated from the relation: $\mu^2 = \mu^2_{1b} x_{1b}$. Its values are shown in Table 2. Comparison of the dipole results in vacuum and in solutions of different polarity indicates a distinct solvent dependence of μ. This environmental effect is caused by an increase in the population of the polar **1b** conformer with increasing dielectric permittivity ε of the medium. Confirmation of the source of the solvent effect is its lack in the case of acetophenone itself (see the last column of Table 2). Nevertheless, one may object that the dipole method, being a macroscopic one, is not able to discriminate the two conformers in equilibrium. Thus, in the next section we shall try to confirm the dipolar data using infrared spectroscopy.

Infrared Spectra of 1,3,5-Triacetylbenzene

The DFT calculations show that the two conformers of **1** are weakly discriminated by their infrared spectra. In this discussion we shall not analyze the whole spectrum, but only those of its regions which can be used for the quantitative estimation of the conformational equilibrium. Therefore, first the two doublets in Table 3 which will further serve as indicators of

Table 3. Position (wavenumber/cm^{-1}) of selected infrared bands of 1,3,5-triacetylbenzene in different environments

Medium	Bands I		Bands II	
	1a	**1b**	**1a**	**1b**
Vacuum			947(38)	942(27)
($B3LYP$/6-311G**)	917(25)	892(15)	947(38)	957(41)
Ar matrix	908	895	964	975
Solid		907		941
				957
CCl$_4$	902.5	892.5	968.5	982
1,2-Dichloroethane	901.5	895	970.5	983.5

In parenthesises are the DFT intensities (km/mol)
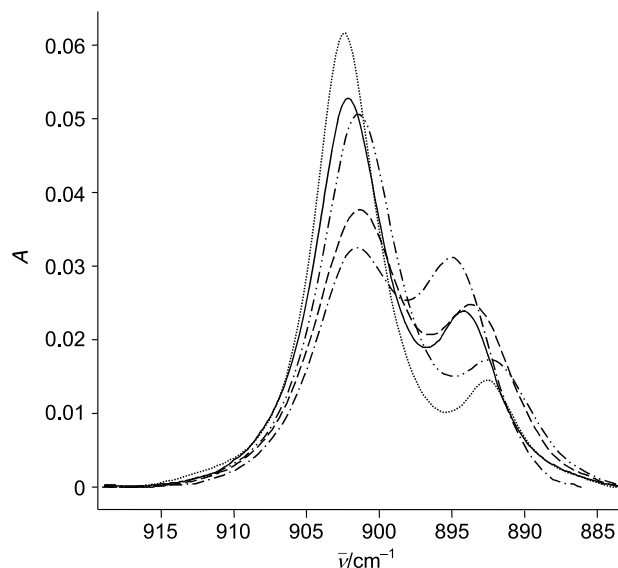

Fig. 1. Infrared spectra in the region between 890 and 905 cm^{-1} of 1,3,5-triacetylbenzene in various solvents; ····· CCl$_4$, − ·· − benzene, — chloroform, − · − 1,2-dichloroethane, and − − − 1,2-dibromoethane (KBr, $l = 0.054$ and 0.264 mm; $c \approx 0.02$–$0.07\,M$)

the position of the **1a** ⇌ **1b** equilibrium in solution are characterized. All these bands are located below 1000 cm^{-1}. They can be assigned to the deformational modes of the ring or the methyl group. The most convincing are two well-separated bands appearing in the solution spectra between 885 and 915 cm^{-1} (bands I). In Fig. 1 the solvent evolution of this doublet is demonstrated. It is seen that an increase in solvent polarity leads to a diminution of the high-wavenumber component with simultaneous intensification of the low-wavenumber band. This behavior is in agreement with DFT calculations, which attribute the first band to the non-polar **1a** conformer and the second to the polar **1b** form (see Table 3). This doublet is also preserved in the matrix spectrum. The second doublet (bands II) is less spectacular because of the contribution arising from both forms to one of its components. The spectra of **1** in the region between 950 and 1000 cm^{-1} and in selected solvents are shown in Fig. 2. The DFT calculations predict four medium-intensive bands in this region. They are attributed to the rocking vibrations of the methyl groups. The DFT band at 957 cm^{-1} can be attributed solely to **1b**. Its experimental analog in the Ar matrix and in the solution spectra is that occurring at 975 and 982–986 cm^{-1}.
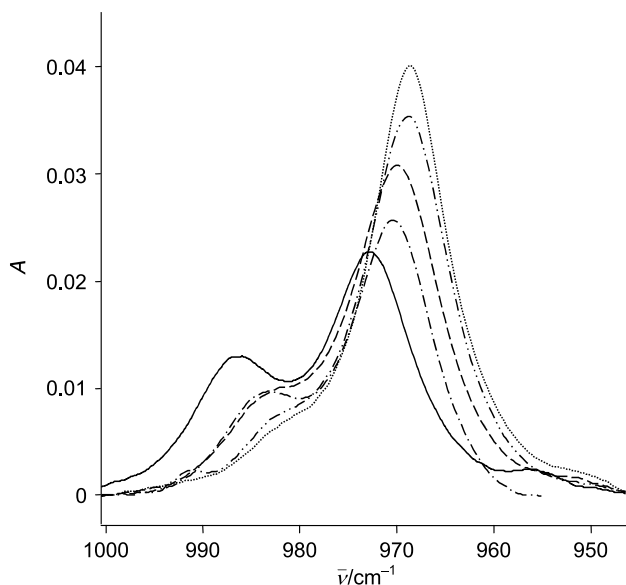
Fig. 2. Infrared spectra in the range between 965 and 985 cm^{-1} of 1,3,5-triacetylbenzene in various solvents; ····· CCl$_4$, − ·· − benzene, — acetonitrile, − · − 1,2-dichloroethane, and − − − 1,2-dibromoethane (KBr, $l = 0.054$ and 0.264 mm; $c \approx 0.02$–0.07 M)

On the other hand, the low-wavenumber component contains the $\rho(CH_3)$ modes arising from both conformers (see Table 3). Nevertheless, this region can also be used to estimate the populations and standard *Gibbs* energy of the conformational equilibrium.

The Position of the 1a ⇌ 1b Equilibrium in Different Environments

The solvent (phase) influence on the **1a ⇌ 1b** transformation can be discussed in terms of the standard

Gibbs energy, $\Delta G^{\rm o}$, of this process. To calculate the $\Delta G^{\rm o}$ energies from the dipolar data, it was assumed that the **1b** conformer contributes a moment of $\mu_{\bf 1b} = 4.47$ D to the experimental dipole moment of **1** in solution. This value was obtained by vectorial summation of the average dipole moments of acetophenone in a few solvents (see Table 2) [7]. The dipole moment of the COCH$_3$ group acts at an angle of 49° to the C$_{\rm ar}$–C bond. Then the so-called dipolar *Gibbs* energy, $\Delta G^{\rm o}(\mu)$, was calculated from the relation: $\Delta G^{\rm o}(\mu) = -RT \ln[\mu^2/(\mu^2_{\bf 1b} - \mu^2)]$. The so-called infrared *Gibbs* energies, $\Delta G^{\rm o}({\rm IR})$, were calculated assuming the DFT molar absorption coefficients of both forms (see Table 3). The $\Delta G^{\rm o}({\rm IR})$ energy in the case of doublet I is therefore defined simply as $\Delta G^{\rm o}({\rm IR}) = -RT \ln(A_{\bf 1b}\varepsilon_{\bf 1a}/A_{\bf 1a}\varepsilon_{\bf 1b})$. When modes arising from both conformers contribute to a given band (doublet II), their concentrations were determined by solving the system of equations. The precision is judged to be 0.20 kJ/mol both in $\Delta G^{\rm o}(\mu)$ and $\Delta G^{\rm o}({\rm IR})$. The $\Delta G^{\rm o}$ energies are collected in Table 4. Since the $\Delta G^{\rm o}$ values obtained by both methods are close, their average value given in Table 4 as $\Delta\overline{G}^{\rm o}$ shall be used in the discussion. Table 4 shows immediately that the $\Delta\overline{G}^{\rm o}$ energy decreases with increasing dielectric permittivity of the medium. In the polar solvents 1-chlorobutane and 1,2-dichloroethane, the polar conformer **1b** starts to dominate ($\Delta\overline{G}^{\rm o} < 0$). It is obvious that, owing to the large magnitude of the dipole moment of **1b**, its dipolar interaction with the solvent should control the position of the **1a ⇌ 1b** equilibrium in the solution. The simplest model describing this interaction is that offered by the continuum-homogeneous di-

Table 4. Experimental *Gibbs* energies of the **1a ⇌ 1b** conformational equilibrium in different environments

Medium	ε	$\Delta G^{\rm o}(\mu)^*$	$\Delta G^{\rm o}({\rm IR})$	$\Delta G^{\rm o}({\rm IR})$	$\Delta\overline{G}^{\rm o}$
Ar matrix			2.77	2.49	2.63
CCl$_4$	2.228	2.71	2.32	2.53	2.52
C$_2$Cl$_4$	2.276	2.47			2.47
1,4-Dioxane	2.219	0.88			0.88
Benzene	2.274	1.78	1.38	1.96	1.71
Mesitylene	2.289	2.24			2.24
Trichloroethylene	3.395	1.58			1.58
1,2-Dibromoethane	4.824	1.05	−0.24	0.80	0.54
Chloroform	4.762		0.68	1.19	0.94
1-Chlorobutane	7.077	−0.28	−0.72		−0.50
1,2-Dichloroethane	10.335	−1.36	−1.17	0.19	−0.78
Acetonitrile	36.01			−1.32	−1.32

* ΔG in kJ/mol
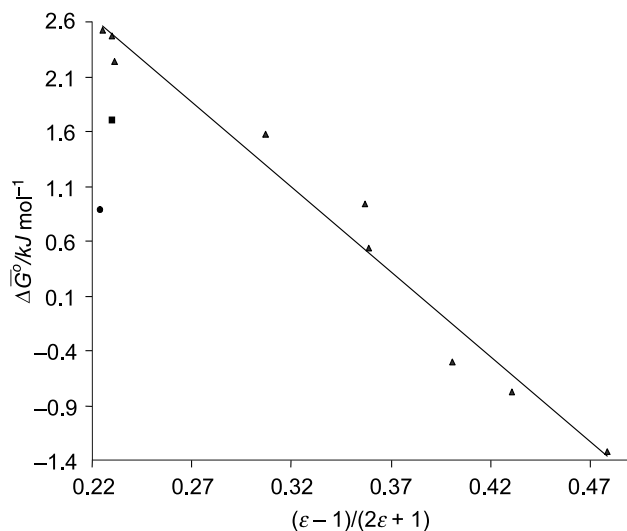
Fig. 3. Relationship between the standard *Gibbs* energy, $\Delta\overline{G}^{\,\mathrm{o}}$, of the $\mathbf{1a} \rightleftharpoons \mathbf{1b}$ conformational equilibrium and the *Onsager-Böttcher* reaction field factor $f(\varepsilon) = (\varepsilon - 1)/(2\varepsilon + 1)$; ■ – benzene ● – 1,4-dioxane, and ▲ – other

electric medium approach. If we simplify the molecule of the **1b** form to a non-polarizable point dipole located in the center of a spherical solvent cavity, then the dipolar contribution to the conformational *Gibbs* energy is [10–13]:

$$\Delta G_{\mathrm{dip}}^{\mathrm{o}} = -N_{\mathrm{A}} \frac{\mu_{\mathbf{1b}}^2}{a_{\mathbf{1b}}^3} f(\varepsilon) \qquad (1)$$

where $a_{\mathbf{1b}}$ is the radius of the spherical cavity and the reaction field factor $f(\varepsilon)$ is $(\varepsilon - 1)/(2\varepsilon + 1)$. The dependence of $\Delta\overline{G}^{\,\mathrm{o}}$ on the reaction field factor is demonstrated in Fig. 3. This figure shows that 1,4-dioxane and, to a lesser extent, benzene behave as solvents characterized by higher polarity than would follow from their bulk ε. An anomalous influence of both solvents in various conformational studies has been already mentioned [14–16]. The strong solvation power of 1,4-dioxane results from its chair $\rightleftharpoons$ boat conformational flexibility. On this basis, an effective ε ranging from 6.4 to 7.7 has been proposed [15]. When both the above solvents are omitted in the relation $\Delta\overline{G}^{\,\mathrm{o}}$ *vs.* $f(\varepsilon)$, then the linear equation assumes the form:

$$\Delta\overline{G}^{\,\mathrm{o}} = 6.04(\pm 0.33) - 15.44(\pm 0.97)f(\varepsilon) \qquad (2)$$

with the correlation coefficient equal to 0.99. However, the validity of the discussed model must be checked not only by the linearity of the $\Delta\overline{G}^{\,\mathrm{o}}$ *vs.* $f(\varepsilon)$ relation, but above all by the agreement of the experimental and theoretical coefficients in Eq. (2).

The theoretical slope of the straight line depends on the choice of the radius of the solvent cavity. Usually we relate its value with the apparent molar volume of the solute [6–9, 17, 18]. The average molar volume of **1** in the solvents under investigation is $175.0\,\mathrm{cm}^3/\mathrm{mol}$. This volume yields a radius of $4.11\,\text{Å}$, characterizing, however, a mixture of **1a** and **1b**. Thus, in the calculations we adopted the radius as being half of the largest interatomic distance in **1b** ($r(\mathrm{HH}) = 9.34\,\text{Å}$). This value, together with $\mu_{\mathrm{B}} = 4.47\,\mathrm{D}$, leads to a predicted slope of 11.82. The intercept of the experimental straight line can be identified with the calculated *Gibbs* energy in vacuum ($\varepsilon = 1$) or the experimental energy in the vapor phase. The theoretical *Gibbs* energies are in the range between 4.90 (PM3) and $7.61\,\mathrm{kJ/mol}$ (DFT) in which the value of $6.04\,\mathrm{kJ/mol}$ exactly extrapolated to $f(\varepsilon) = 0$ is located.

Concluding, this simple continuum-homogeneous dielectric model quite well explains the solvent dependence of the conformational equilibrium in **1**. On the other hand, the $\Delta G^{\mathrm{o}}(\mathrm{IR})$ values obtained from the Ar matrix spectra are markedly lower than those in vacuum. They are comparable with the $\Delta\overline{G}^{\,\mathrm{o}}$ energy obtained in CCl_4 ($\varepsilon = 2.228$). It seems that clustering of the **1** molecules increases the population of the polar **1b** conformer in relation to the isolated molecule.

Methods

Electric dipole moments were determined with the equipment previously described [6–9]. All measurements were performed at $298\,K$. The molar dipole polarization of the solute (P) was obtained within the framework of the *Onsager* reaction field model [10]. After its extrapolation to an infinite dilution of the solution, the molar dipole polarization ($P_{2\infty}$) is given by the expression [19]:

$$P_{2\infty} = \frac{(2\varepsilon_1 + n_1^2)(\varepsilon_1 - n_1^2)M_1}{\varepsilon_1(n_1^2 + 2)^2 d_1}$$
$$\times \left(\frac{\alpha\varepsilon_1 - \gamma n_1^2}{\varepsilon_1 - n_1^2} + \frac{2\alpha\varepsilon_1 + \gamma n_1^2}{2\varepsilon_1 + n_1^2} - \frac{2\gamma n_1^2}{n_1^2 + 2} - \alpha - \beta + \frac{M_2}{M_1} \right)$$
$$(3)$$

where ε, d, n, and M are dielectric permittivity, density, refraction index, and molecular mass. The coefficients $\alpha\varepsilon_1$, β, and γn_1^2, demonstrated in Table 2, were defined as:

$$\alpha\varepsilon_1 = \left(\frac{d\varepsilon_{12}}{dx_2} \right)_{x_2 \to 0}; \qquad \beta d_1 = \left(\frac{dd_{12}}{dx_2} \right)_{x_2 \to 0};$$
$$\gamma n_1^2 = \left(\frac{dn_{12}^2}{dx_2} \right)_{x_2 \to 0} \qquad (3.1)$$

The subscripts 1 and 2 describe the solvent and solute. The formula for calculating the dipole moment at $298\,K$ is: $\mu = 0.21986\sqrt{P_{2\infty}}$. The average of the absolute deviations of the dipole moments from their mean, usually determined for six different concentrations, did not exceed 0.03 D.

The experimental equipment used for preparing the matrix samples was described in detail previously [20, 21]. Briefly, the solid compound was evaporated from a recently developed movable mini-oven placed in the cryostat. The optimal sublimation temperature was found to be 301 K. The vapor of the product, mixed with a large excess of Ar gas, was deposited onto the cold CsI window (maintained at 11 K). The IR spectra of the matrix as well as the solid **1** in KBr pellets were recorded with a Bruker IFS-66 *Fourier* transform instrument at a resolution of $1\,cm^{-1}$. The infrared spectra of **1** in different solvent were collected for solutions with concentrations between 0.02 and $0.07\,mol/dm^3$ and in KBr cells of 0.264 and 0.054 mm thickness on a Nicolet 205 FT-IR spectrophotometer with the same resolution as above. The infrared spectra were baseline and offset corrected as well as solvent subtracted by the Grams 32 program (Galactic Inc., Salem, NH). 1,3,5-Triacetylbenzene (CHEMPUR, Karlsruhe) was purified by recrystallization from acetone. All solvents were purified by standard methods [22] and dried over $4\,\text{Å}$ molecular sieves.

The geometry of the studied conformers of **1** were optimized using the DFT method. A hybrid of *Becke*'s non-local three-parameter exchange and correlated functional with the *Lee–Yang–Parr* correlation functional (*B3LYP*) was used [23–25]. The 6-311G** basis set was employed to represent the molecular orbitals. The infrared frequencies and intensities were computed at the same level of theory using the harmonic approximation and the analytical derivative procedure incorporated in the Gaussian 98 program [26]. Theoretically predicted frequencies were scaled down using a uniform scaling factor of 0.97. Assignment of the theoretical frequencies was performed by animation of molecular vibrations with the MOLDEN program [27]. For PM3 and AM1 molecular modeling, which was performed in addition to the DFT method, Hyperchem software (Hypercube Inc.) was used.

Acknowledgements

References

[1] Exner O (1975) Dipole Moments in Organic Chemistry, Thieme, Stuttgart

[2] Cure J, Liegeois Ch, Lumbroso H (1978) Bull Soc Chem France **7**/**8**: 323

[3] Oconnor BH, Moore FH (1973) Acta Cryst **B29**: 1903

[4] Oconnor BH (1973) Acta Cryst **B29**: 1893

[5] Semenkovich GV, Strokach NS, Shigorin DN (1988) Zh Fiz Khim **62**: 1272

[6] Konopacka A, Kalenik J, Pawełka Z (2004) J Mol Struct **705**: 75

[7] Konopacka A, Filarowski A, Pawełka Z (2005) J Solution Chem **34**: 929

[8] Konopacka A, Pawełka Z (2005) J Phys Org Chem **18**: 1190

[9] Konopacka A, Pająk J, Jezierska A, Panek J, Ramaekers R, Maes G, Pawełka Z (2006) Struct Chem **17**: 177

[10] Onsager L (1936) J Am Chem Soc **58**: 1486

[11] Böttcher CJF (1952) Theory of Electric Polarization, Elsevier, Amsterdam

[12] Abraham RJ, Bretschneider E (1974) Internal rotation in molecules. In: Orville-Thomas WJ (ed) Wiley, London, Chapter 13

[13] Małecki J (1982) Molecular interactions. In: Ratajczak H, Orville-Thomas WJ (eds) vol. III. Wiley, London

[14] Abraham RJ, Siverns TM (1972) J Chem Soc Perkin 2 1586

[15] Eliel EL, Hofer O (1973) J Am Chem Soc **95**: 8041

[16] Geerhing JD, Varma CAGO, van Hemert MC (2000) J Phys Chem **B104**: 56

[17] Pawełka Z (1988) J Mol Struct **172**: 15

[18] Pawełka Z (1988) J Mol Struct **178**: 161

[19] Pawełka Z (1988) J Chem Soc Faraday Trans 2 **84**: 1683

[20] Maes G (1981) Bull Soc Chem Belg **90**: 1093

[21] Graindourze M, Smets J, Zeegers-Huyskens Th, Maes G (1990) J Mol Struct **222**: 465

[22] Weissberger A, Proskauer ES, Riddick JA, Tops EE (1955) Technique of Organic Chemistry, Organic Solvents, vol. VII. Interscience, New York

[23] Lee C, Yang W, Parr RG (1988) Phys Rev **B37**: 785

[24] Becke AD (1993) J Chem Phys **98**: 5648

[25] Parr RG, Yang W (1989) Density-Functional Theory of Atoms and Molecules, Oxford University Press, New York

[26] Frisch MJ, Trucks GW, Schlegel HB, Scuseria GE, Robb MA, Cheeseman JR, Zakrzewski VG Jr, Montgomery JA, Stratmann RE, Burant JC, Dapprich S, Millan JM, Daniels AD, Kudin KN, Strain MC, Farkas O, Tomasi J, Barone V, Cossi M, Cammi R, Mennucci B, Pomelly C, Adamo' C, Clifford S, Ochterski J, Petersson GA, Ayala PY, Cui Q, Morokuma K, Malick DK, Rabuck AD, Raghavachari K, Foresman JB, Cioslowski J, Ortiz JV, Baboul AG, Stefanov BB, Liu G, Liashenko A, Piskorz P, Komaromi I, Gomperts R, Martin RL, Fox DJ, Keith T, Al-Laham MA, Peng CY, Nanayakkara A, Gonzalez C, Challacombe M, Gill PMW, Johnson B, Chen W, Wong MW, Andres JL, Gonzalez C, Head-Gordon M, Replogle ES, Pople JA (1998) Gaussian 98, Rev A5 programme, Gaussian Inc., Pittsburgh, PA

[27] Schaftenaar G, Noordik JH (2000) J Comp Aided Mol Design, **14**: 123